Journal of Materials Chemistry

Dynamic Article Links

Cite this: J. Mater. Chem., 2012, 22, 3578

www.rsc.org/materials

PAPER

Segregation at a small scale: synthesis of core–shell bimetallic RuPt nanoparticles, characterization and solid state NMR studies†

Patricia Lara,[ab] Marie-José Casanove,[cd] Pierre Lecante,[cd] Pier-Francesco Fazzini,[e] Karine Philippot*[ab] and Bruno Chaudret*[e]

Received 23rd September 2011, Accepted 9th December 2011
DOI: 10.1039/c2jm14757b

Core–shell small RuPt nanoparticles stabilized by a polymer (polyvinylpyrrolidone, PVP) have been prepared by co-decomposition of [Ru(COD)(COT)] [(1,5-cyclooctadiene)(1,3,5-cyclooctatriene) ruthenium] and [Pt(CH_3)$_2$(COD)] [dimethyl(1,5-cyclooctadiene)platinum(II)] organometallic complexes at room temperature. The control of the metal segregation is made possible by the difference in the decomposition temperature of the metal precursors, giving rise to a heterogeneous nucleation process. The structural composition of these nanoparticles has been determined by a combination of techniques (TEM, HREM, WAXS, EXAFS, STEM-HAADF, IR, NMR). In particular, after adsorption of ^{13}CO as a probe molecule, solid-state NMR investigation provided useful information on the chemical segregation in these nanoparticles.

Introduction

Bimetallic nanoparticles are attractive materials in many fields ranging from physics (hard or soft magnetic materials, …) to catalysis (heterogeneous catalysts for difficult hydrogenations, electrocatalysts for fuel cells, …).[1] In all cases the control of the chemical order within the particle is crucial, especially when only one given defined compound gives rise to the wanted property as in FePt.[2] However, it can be of interest to control the segregation within a single particle, for example to expose a small quantity of precious catalytic metal or to modify the magnetic properties. For large particles (>5 nm), the control of the chemical order is well documented but for small particles, a core–shell structure may mean the deposition of one monolayer or less of a metal onto another one. For example, in the case of face-centred cubic (fcc) Pt nanoparticles, a diameter of approximately 1.6 nm corresponds to a magic number of 147 with almost two-thirds of atoms at the surface. In this case, a phase segregated bimetallic particle, for example of PtRu, would contain less than one monolayer of one metal on the other.

Such a precise control is difficult by chemical means but can be achieved by employing smooth procedures such as the organometallic method we have developed over 20 years.[3] In this case, the organometallic precursor is decomposed by a reactive gas (H_2 or CO) under mild conditions (room temperature; $P = 3$ bar). As a result, a good control of the surface chemistry is obtained and the presence of surface hydrides on ruthenium nanoparticles has been demonstrated.[4] Using such an organometallic procedure, we have studied 10 years ago the preparation of bimetallic RuPt nanoparticles by hydrogenation of a mixture of [Pt(dba)$_2$] (bis-(dibenzylideneacetone)platinum) and [Ru(COD)(COT)] [(1,5-cyclooctadiene)(1,3,5-cyclooctatriene)ruthenium] as metallic precursors.[5] In that work, the synthesis and structural characterization of RuPt nanoparticles containing different metal ratios and stabilized by the polymer PVP were reported. We could thus prepare alloyed nanoparticles which adopted the fcc structure of platinum up to the composition Pt_1Ru_3 after which, for a higher content of Ru, the hexagonal close-packed (hcp) structure was found. Interestingly, at the precise composition Pt_1Ru_3, a large majority of the particles were twinned. This study showed that despite their respective structure, it was possible to obtain small alloyed nanoparticles involving Ru and Pt. More recently, using a kinetic control, it has been possible to prepare segregated *ca.* 2 nm Rh@Fe nanoparticles by hydrogenation of a mixture of Fe[N(SiMe$_3$)$_2$]$_2$ and Rh(η^3-C_3H_5)$_3$.[6] However, the two precursors are very different and some intermixing of Fe and Rh layers has been deduced from structural studies.

Having progressed in the field of synthesis and in surface characterization, in particular using NMR[4b] and microscopy techniques, we decided to apply our method to try to deposit a monolayer of one metal onto another. We considered RuPt since we already know this bimetallic system which is of high

[a]*CNRS, LCC (Laboratoire de Chimie de Coordination), 205, Route de Narbonne, F-31077 Toulouse, France. E-mail: karine.philippot@lcc-toulouse.fr; Fax: +33561553003; Tel: +33561333230*
[b]*Université de Toulouse, UPS, INPT, LCC, F-31077 Toulouse, France*
[c]*CNRS, CEMES (Centre d'Elaboration de Matériaux et d'Etudes Structurales), BP 94347, 29 rue Jeanne Marvig, F- 31055 Toulouse, France*
[d]*Université de Toulouse, UPS, F-31055 Toulouse, France*
[e]*LPCNO, Laboratoire de Physique et Chimie de Nano-Objets, 135, Avenue de Rangueil, F-31077 Toulouse, France. E-mail: chaudret@insa-toulouse.fr; Fax: +33561559697; Tel: +33561559655*
† Electronic supplementary information (ESI) available. See DOI: 10.1039/c2jm14757b

interest in many applications, especially regarding fuel cell catalysts.[1] As precursors, we chose [Ru(COD)(COT)] and [$Pt(CH_3)_2$(COD)] [dimethyl(1,5-cyclooctadiene)platinum(II)]. This choice was made knowing that [$Pt(CH_3)_2$(COD)] does not decompose at room temperature under H_2 while [Ru(COD)-(COT)] does. In this way we hoped to proceed only through heterogeneous nucleation and hence smoothly deposit platinum onto preformed ruthenium nanoparticles. The particles were characterized by a combination of methods including TEM, HREM, WAXS, EXAFS, STEM-HAADF, infrared and NMR spectroscopy after adsorption of ^{13}CO as a probe molecule of their surface chemistry.

Results and discussion

A series of bimetallic nanoparticles was synthesized by decomposing [Ru(COD)(COT)] and [$Pt(CH_3)_2$(COD)] (in a relative ratio of 1 : 1) in the presence of PVP and using different metal concentrations relative to the solvent. The decomposition was carried out under 3 bar of H_2. A color change was observed immediately but the reaction was left stirring for 3 days for completion. Then a black precipitate formed which was purified by washings with pentane and evaporation to dryness (see Scheme 1).

Two samples were prepared following these conditions: **Colloid 1** using a concentration of 8.3 mM for each metal and **Colloid 2** using a concentration of 2 mM for each metal. The size and the structure of the particles were characterized by TEM (transmission electron microscopy), WAXS (wide angle X-ray scattering), EXAFS (extended X-ray absorption fine structure), HREM (high resolution electron microscopy) and STEM-HAADF (scanning transmission electron microscopy using a high angle annular dark field detector).

TEM analysis of these 2 samples shows crystalline and monodisperse nanoparticles with a mean size of respectively 2.8 (0.3) and 2.8 (0.5) nm for **Colloids 1** and **2** (see Fig. 1 for a representative example of **Colloid 1** and Fig. S1† for **Colloid 2**, respectively). ICP-MS (Inductively Coupled Plasma-Mass Spectrometry) performed on purified samples of **Colloids 1** and **2** confirms the presence of both metals in a relative ratio Ru : Pt of 1.1 : 1 and 1.05 : 1 respectively, very close to the expected theoretical values.

In order to fully understand the chemical order within one particle, three complementary approaches were used: X-ray techniques (WAXS and EXAFS) which bring an average characterization of the whole sample, electron microscopy techniques

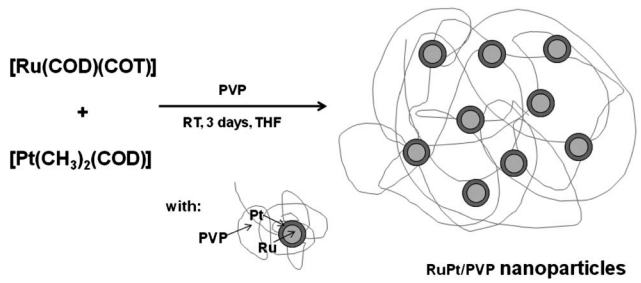

Scheme 1 Reaction conditions used for the synthesis of RuPt nanoparticles.

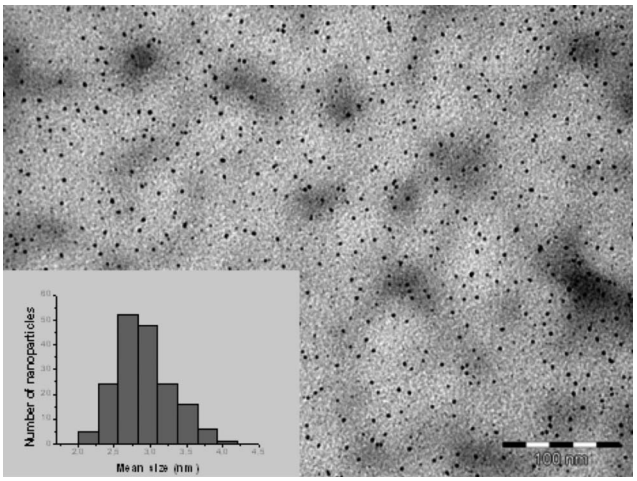

Fig. 1 TEM image with the corresponding size histogram of **Colloid 1**.

(HREM and STEM-HAADF) which offer a detailed characterization of selected objects and spectroscopy techniques which characterize the surface species.

X-Ray techniques

WAXS studies afford the RDF functions of the different colloids. **Colloids 1** and **2** are fully identical (see Fig. 2, superposed RDFs in the middle). Their coherence lengths, which are by principle average measurements of crystalline domains, can be evaluated to 2.6 nm, in good agreement with mean sizes derived from TEM analysis. This is a strong indication that the nanoparticles are fully crystalline. When compared to simulated RDFs based on perfect Pt fcc or Ru hcp structures (Fig. 2, top and bottom, respectively), strong deviations can however be observed. Using characteristic patterns at 0.6 and 1.0 nm as markers for the model structures, we can estimate that these particles are much closer to the fcc organization than to the hcp one.

In order to have detailed information concerning the environment of Pt and Ru atoms in these NPs, EXAFS measurements were carried out on **Colloid 2**. Pure Pt and Ru

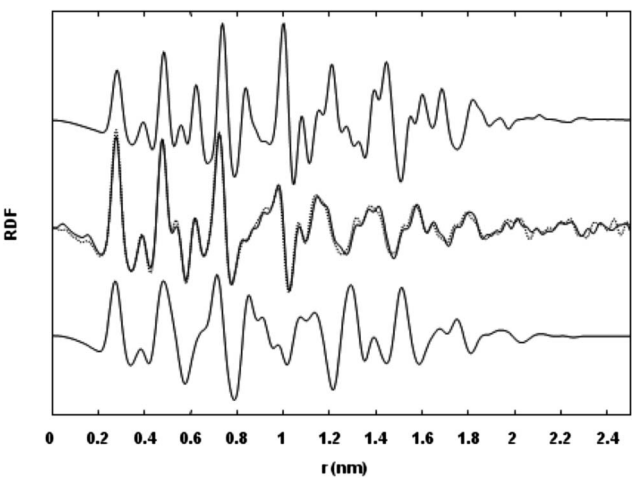

Fig. 2 WAXS analysis of **Colloids 1** and **2** (middle: superposed RDFs obtained) and for comparison, RDFs simulated from fcc (top) and hcp (bottom) structures.

nanoparticles were also measured under the same conditions. At the Pt LIII absorption edge, the EXAFS function and related Fourier transform (Fig. 3, top) from pure Pt NPs can be fitted using parameters from bulk metal, taking into account a small bond length reduction (0.272 nm *vs.* 0.277 nm) and a significant amplitude reduction related to both size and disorder effects. This is not the case for **Colloid 2**: oscillations are cancelled in the middle of the EXAFS function, which indicates a drastic change in the Pt local environment. The best agreement was reached using a mixed environment: 8 Pt atoms at 0.273 nm and 4 Ru atoms at 0.270 nm with similar values for disorder. Actually, slightly different environment values can be obtained allowing for individualized disorders, but they all point to a well defined local order around Pt atoms including a minor amount of Ru.

At the Ru K absorption edge, the quality of collected data is much worse. The fit presented was obtained using only Ru atoms as environment, since it was not possible to obtain a stable fit when introducing Pt atoms. However, the very poor agreement, especially near 6 $Å^{-1}$, likely indicates also a mixed environment for Ru atoms. Static structural disorder is clearly much higher for the Ru-rich part of the sample.

These elements are consistent with a model where most of the Pt atoms are engaged in a locally well-ordered Pt-rich phase and most Ru atoms in a disordered Ru-rich one, in other words a partially segregated Pt/Ru alloy. They however do not provide a clear localization of the Pt-rich and Ru-rich components.

Electron microscopy techniques

HREM analyses of **Colloids 1** and **2** (see Fig. 4 and 5, respectively) show that the particles have roughly the same size (*ca.* 2.5–2.7 nm)

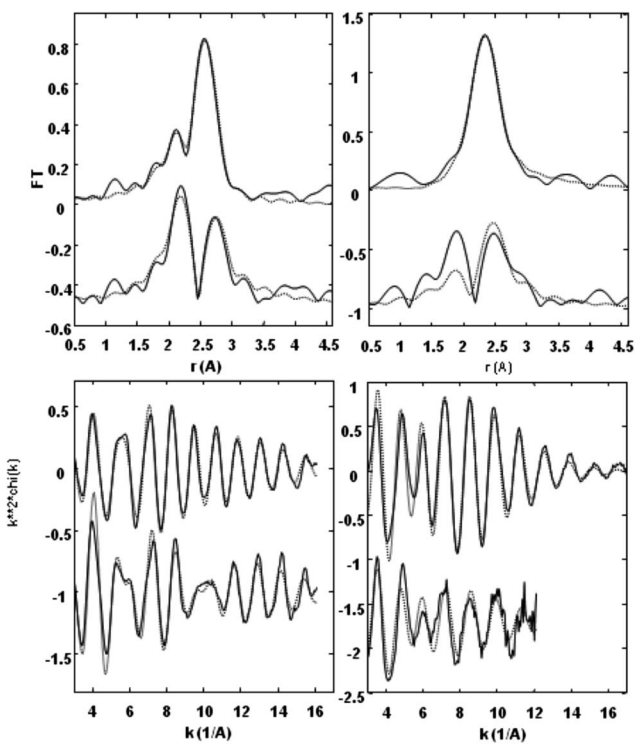

Fig. 3 EXAFS functions (bottom) and related Fourier transforms (top) at Pt LIII (left) and Ru K (right) absorption edge of pure Pt (Ru) NPs, **Colloid 2** (from top to bottom).

and that most particles display a fcc structure, although many of them include twins or stacking faults. In the case of **Colloid 2**, some particles even exhibit 5-fold symmetry axes, characteristic of icosahedral or decahedral particles, as in Fig. 5.

In all the studied samples, the nanoparticles are not perfectly crystalline. Most of them display twin boundaries or stacking faults, which is consistent with the deviation to the perfect fcc or hcp structure observed by WAXS. Interestingly, this is in contrast to the results obtained in our previous work on RuPt particles of the same composition but synthesized using different precursors.[5] This could result from segregation of the two metals, which is in agreement with both kinetic (in the present case, kinetics of decomposition of the precursors) and thermodynamic considerations. Indeed, from a thermodynamic point of view, although the growth conditions of the synthesis do not favor the onset of a thermodynamic equilibrium, different driving forces such as the difference in surface energy of the two elements (platinum has a much lower surface energy than ruthenium) or in the atomic size (platinum atom is larger than ruthenium atom) could lead to segregation of platinum at the surface of the particle, while ruthenium would concentrate at the particle core.

The distribution of the different elements (platinum and ruthenium) inside a particle could be analyzed, at least in principle, by different techniques providing elemental mapping (for instance, energy dispersive X-ray spectroscopy in STEM mode (STEM/EDS) or techniques based on electron energy loss spectroscopy (EELS) as energy filtered TEM (EFTEM) and STEM/EELS), but the very small size of our particles prevents such analyses (too long exposure time would be necessary with regard to the stability of the particles and carbon foil under an electron beam). To circumvent this problem, we used the HAADF technique to prove the phase segregation. The image contrast obtained by the HAADF technique when imaging particles is proportional to the local thickness of the particle multiplied by the atoms' Z number. By this way, we could confirm that the different atoms in the particles are segregated. Since the particles are thicker in the center, the experimental results (see Fig. 6) clearly show the presence of heavy atoms (Pt) at the periphery and lighter atoms (Ru) in the core.

Surface investigations

In our previous study[5] concerning RuPt nanoparticles prepared by hydrogenating a mixture of [Ru(COD)(COT)] and [$Pt(dba)_2$],

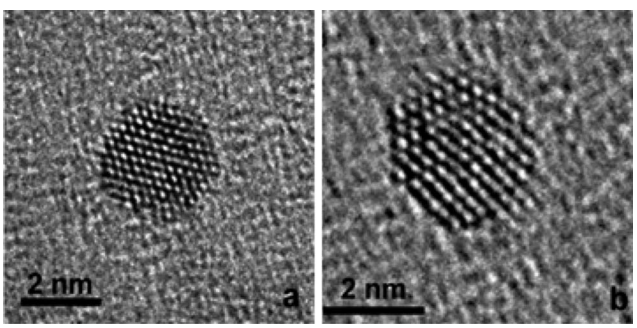

Fig. 4 HREM micrographs of **Colloid 1** showing two different particles with (a) nearly perfect fcc structure and (b) faulted fcc structure.

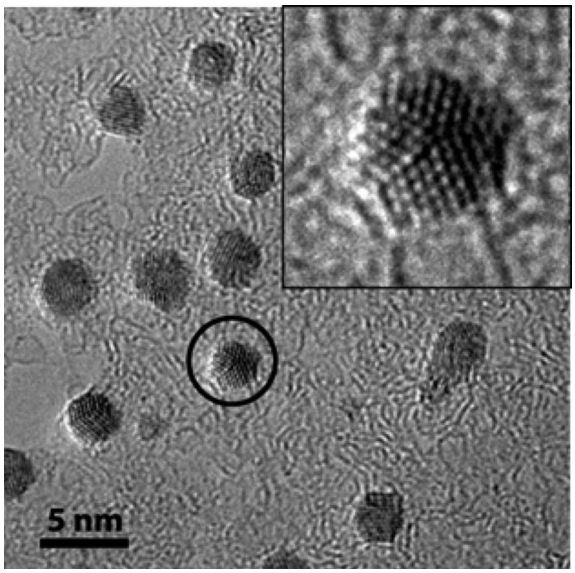

Fig. 5 HREM micrograph of **Colloid 2** showing well-dispersed particles. The circled particle (also displayed in the inset) presents a five-fold symmetry axis.

the particles were smaller (1.5 nm) and only *ca.* 20% of them were twinned. The WAXS and HREM analyses concluded that most particles were not segregated but displayed a statistical distribution of both metals as in alloys. In the present case using another platinum precursor, the results obtained from X-ray and microscopy techniques are different from these previous ones.[5b] This led us to consider complementary techniques to pursue our investigation. We have recently developed the investigation of the surface of nanoparticles, in particular the location and dynamics of hydrides and CO groups, using a combination of NMR methods and reactivity studies.[4,7] However these studies have been so far limited to ruthenium nanoparticles. It was therefore of interest to determine whether they could be extended to bimetallic systems and whether they could shed some light on the nature of the surface metal atoms.

First of all, as the Pt–H bond is expected to be stronger than the Ru–H one[8] and since this can have an effect on the rate and on the degree of substitution of hydrides by CO, it was necessary to determine whether hydrides were present on RuPt NPs.

Surface hydrides were quantified applying the procedure developed for ruthenium nanoparticles, a titration based on an olefin hydrogenation reaction.[4] In the present case, 2-norbornene was added to a fresh THF solution of RuPt nanoparticles previously pretreated by vacuum/argon cycles to eliminate any trace of dissolved dihydrogen. The conversion of the olefin into norbornane was followed by gas chromatography while no dihydrogen was added, thus taking profit only on the surface hydrides to hydrogenate the double bond. Assuming a size of 2.8 nm for **Colloid 1** which corresponds to *ca.* 45–50% of atoms on the surface (magic fcc number 561), we found *ca.* 1.7 hydrides per surface atom which is coherent for a purely sterically stabilized nanoparticle.[4a,9]

CO has been widely used as an infrared active probe molecule for identifying coordination sites on surfaces and nanoparticles.[10] In addition, we have recently reported that the coordination of ^{13}CO could also lead to a sensitive NMR probe.[4b] Thus, we have shown that CO molecules are dynamic on the surface of ruthenium nanoparticles only sterically stabilized by PVP, whereas the presence of extra ligands prevents exchange between bridging and terminal CO groups.[4b] In contrast, NMR studies on platinum nanoparticles have known to be difficult since the pioneering work of Slichter, because of the presence of an important Knight shift.[11] It is therefore of interest to determine the behavior of CO on bimetallic nanoparticles and explore the possibility of using CO to determine the nature of the surface atoms.

The infrared and MAS NMR spectra of **Colloid 1** do not show any salient feature besides the signals of PVP. However, after exposure to ^{13}CO, we can observe by infrared a band at 1995 cm^{-1} with a shoulder at 1946 cm^{-1} that can be assigned to ^{13}CO coordinated in a linear mode to platinum (see ESI, Fig. S2†). This value which corresponds to 2045 cm^{-1} for ^{12}CO is typical of terminal CO groups linked to platinum, a lower value near 2000–2020 cm^{-1} would be expected for CO on ruthenium.[5a,10a,b,12]

The MAS NMR spectra run after exposure of **Colloid 1** to 0.5 bar ^{13}CO for 5 and 12 h are different from those obtained for pure Ru nanoparticles of *ca.* 2 nm size: the RuPt particles show a broad peak at *ca.* 200 ppm with an even broader signal, centered at *ca.* 240 ppm and finally a broad signal which is not a spinning side band at *ca.* 320 ppm (see Fig. 7 and S5 in the ESI†, respectively). A chemical shift near 200 ppm is typical for a CO group coordinated in a linear mode, in agreement with previous results describing such a coordination mode for CO on platinum.[10b,11,12] For comparison, in the case of Ru nanoparticles, the same experiment leads to the fast substitution of hydrides, and the observation of first only bridging CO groups near 250 ppm.

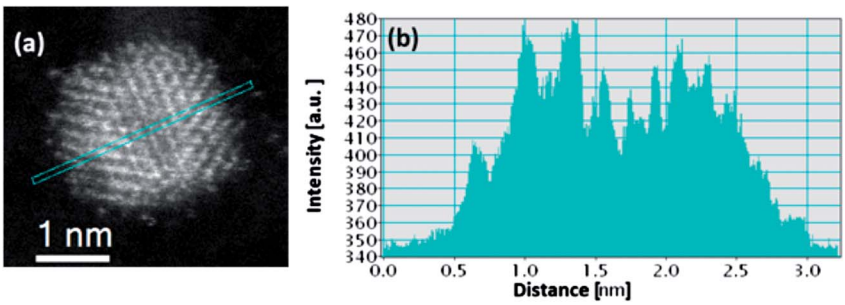

Fig. 6 STEM-HAADF image (a) and intensity profile extracted from the particle center (b) of a RuPt nanoparticle of **Colloid 1**.

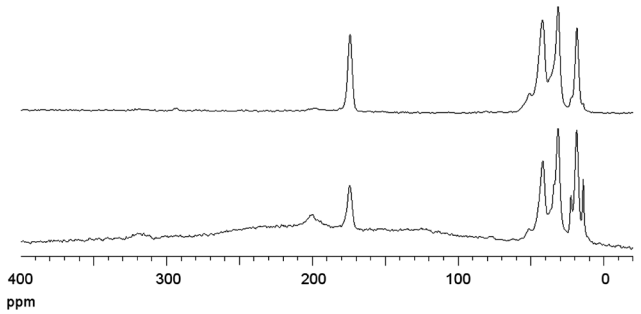

Fig. 7 ^{13}C MAS (bottom) and ^{13}CP MAS (top) NMR spectra obtained for **Colloid 1** after reaction with ^{13}CO (0.5 bar, rt, 5 h).

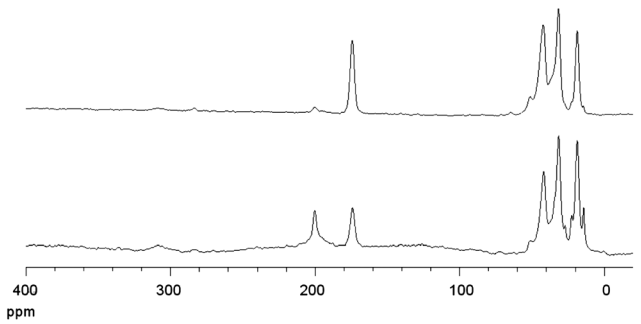

Fig. 8 ^{13}C MAS (bottom) and ^{13}CP MAS (top) NMR spectra obtained for **Colloid 2** after reaction with ^{13}CO (1 bar, rt, 18 h).

If the colloid is exposed for a longer time (18 h) to a higher pressure of ^{13}CO (1 bar), a sharper signal develops at 200 ppm with loss of the bump near 240 ppm but with still a signal near 310 ppm (see Fig. 8). The presence of a single signal near 200 ppm and the absence of spinning side bands indicate that CO is fluxional on the nanoparticle surface. A result somewhat similar is observed on Ru nanoparticles after a long exposure to CO, with a signal at 199 ppm attributed to a fluxional CO group in a linear coordination mode on the surface of the particles. The signals observed after 5 and 18 h appear both weaker when applying the cross-polarization technique, which indicates the absence of hydrogen nearby. The presence of a broad peak at 320 ppm is not explained but could result from CO dissociation on the surface. However the hypothetical resulting carbide is not hydrogenated since this would appear clearly in the CP MAS experiment.

These spectroscopic data are in favor of the coordination of ^{13}CO molecules onto Pt atoms. A difference between the Ru and RuPt systems is that the hydride substitution process is much slower on RuPt NPs. This is presumably due to the necessity to eliminate hydrides from the surface and from the higher Pt–H bond energy compared to the Ru–H one as discussed hereabove.[8]

In summary, both IR and NMR results are in agreement with the coordination of CO to platinum and therefore with the presence of a segregated Ru core/Pt shell structure, and confirm the results obtained by the structural techniques HREM, WAXS, EXAFS and STEM-HAAD.

Conclusions

We report in this paper the preparation of core/shell ruthenium/platinum nanoparticles sterically stabilized by a polymer, namely polyvinylpyrrolidine. The choice of two precursors containing only ligands which are easily eliminated by hydrogenation leads to bimetallic nanoparticles displaying a surface only covered by hydrides. High level solid state techniques suggest the presence of a segregated structure which is confirmed by spectroscopic studies using ^{13}CO as a molecular probe. This is obviously a favorable case since both the kinetic parameters (fast decomposition of [Ru(COD)(COT)], slow decomposition of $[Pt(CH_3)_2(COD)]$) and the thermodynamic parameters (preference for Ru in the core because of higher surface energy and smaller size than Pt) point to the same direction. It however evidences the strength of the alternative organometallic chemistry approach to selectively deposit a monolayer of one metal on top of the other. This study also evidences the complementarity of the structural and molecular approaches for elucidating the structure of very small bimetallic nanoparticles.

Experimental

General procedures and reagents

All operations were carried out using standard Schlenk tubes, Fischer–Porter bottle techniques or in a glove-box under argon atmosphere.

Solvents were purified just before their use: THF (Sigma-Aldrich) by distillation under argon over sodium/benzophenone, pentane (SDS) through filtration on a column in a purification system (Braun). [Ru(COD)(COT)] was purchased from Nanomeps, Toulouse, $[Pt(CH_3)_2(COD)]$ from Strem Chemicals, CO and H_2 from Air liquide, ^{13}CO (^{13}C, 99.14%) from Eurisotop, and polyvinylpyrrolidone (PVP) from Sigma Aldrich; all were used without purification.

RuPt NPs were observed by TEM, HRTEM and STEM-HAADF after deposition of a drop of the crude THF colloidal solution on a covered holey copper grid. TEM analyses were performed at the "Service Commun de Microscopie Electronique de l'Université Paul Sabatier" (TEMSCAN-UPS) by using a JEOL JEM 1011 CX-T electron microscope operating at 100 kV with a point resolution of 4.5 Å. The approximation of the particles' mean size was made through a manual analysis of enlarged micrographs by measuring the number of particles on a given grid. HREM analyses were performed at CEMES by using a FEI Tecnai F20 operated at 200 kV and fitted with a Cs aberration corrector of the objective lens. The resolution of this TEM is as good as 0.12 nm. STEM/HAADF observations have been carried out at the INA institute of Zaragoza, using a Titan Microscope equipped with an XFEG source and a probe Cs corrector.

Wide-angle X-ray scattering (WAXS) was performed at CEMES-CNRS. Samples were sealed in 1 mm diameter Lindemann glass capillaries. The samples were irradiated with graphite-monochromatized molybdenum K_α (0.071069) radiation and the X-ray intensity scattered measurements were performed using a dedicated two-axis diffractometer. Radial distribution functions (RDFs) were obtained after Fourier transformation of the reduced intensity functions.

EXAFS measurements were performed at HASYLAB in Hamburg on beamline C in transmission mode at room temperature. Both Pt LIII and Ru K absorption edges could be

measured for all samples. Data analysis was performed using the Athena software. Least-square refinement of structural parameters could also be performed using the Artemis software.

Solid state NMR (MAS-NMR) analyses with and without ^{1}H–^{13}C cross-polarization (CP) were performed at the LCC on a Bruker Avance 400WB instrument equipped with a 4 mm probe with the sample rotation frequency being set at 12 kHz unless otherwise indicated. Measurements were carried out in a 4 mm ZrO_2 rotor.

Gas chromatography was performed using a HP 5890 Series II Gas Chromatograph with a SGE BP1 non-polar 100% dimethyl polysiloxane capillary column (50 m × 0.32 mm × 0.25 μm). The method used for the quantification of hydrides consists of 15 min at 40 °C and a ramp of 8 °C min^{-1} until 250 °C.

IRFT spectra were recorded on a Perkin-Elmer GX2000 spectrometer in the range 4000–400 cm^{-1}. All the samples were prepared as KBr pellets under argon atmosphere.

ICP analyses were performed at Antellis, Toulouse, and elemental analysis at the LCC.

Samples synthesis

Colloid 1

200 mg of complex [Ru(COD)(COT)] (0.63 mmol) and 211.64 mg of complex [$Pt(CH_3)_2$(COD)] (0.63 mmol) were introduced in a Fischer–Porter bottle and dissolved in 40 mL of THF. A solution containing 1.17 g of polymer PVP in 40 mL of THF was added to the Fischer–Porter bottle at room temperature. The reaction bottle was filled with H_2 (3 bar). A black homogeneous solution was immediately formed and the mixture was stirred for 3 days at room temperature. After this period of time, excess of H_2 was eliminated and solvent was evaporated to dryness. 50 mL of pentane were added to the black residue obtained and evaporated. Nanoparticles were dried overnight in the vacuum line.

ICP analysis: 5.8% (Ru), 10.2% (Pt); elemental analysis: C, 53.8; H, 5.7; N, 9.8%.

Colloid 2

549 mg of PVP were dissolved in 50 mL of THF degassed by three freeze–pump cycles. This colourless solution was transferred to a Fischer–Porter bottle containing a solution of 93.8 mg of complex [Ru(COD)(COT)] (0.298 mmol) and 99.2 mg of [$Pt(CH_3)_3$(COD)] (0.298 mmol) in 100 mL of THF. The reaction bottle was pressurized with 3 bar of H_2. A black homogeneous solution was immediately formed and the mixture was stirred for 3 days at room temperature. After this period of time, the H_2 was evacuated and solvent was evaporated to dryness. 50 mL of pentane are added to the black residue obtained and subsequently evaporated. Nanoparticles were dried overnight in the vacuum line.

ICP analysis: 4.5% (Ru), 8.8% (Pt); elemental analysis: C, 55.8; H, 7.6; N, 9.8%.

Quantification of surface hydrides

A solution of freshly prepared PtRu nanoparticles was submitted to 5 cycles of 1 minute vacuum/1 minute argon in order to eliminate any hydrogen dissolved in the THF. Then, 2-norbornene was added (5 equiv.) and its conversion into 2-norbornane was monitored by injecting free NP solutions (after filtration with Al_2O_3 and cotton) in a GC. Assuming a size of 2.8 nm for **Colloid 1** which corresponds to *ca.* 45 to 50% atoms on the surface (magic fcc number 561), we found *ca.* 1.7 hydrides per surface atom which is coherent for a purely sterically stabilized nanoparticle.

Reactions with CO

The coordination of carbon monoxide on the surface of the RuPtPVP nanoparticles was performed as follows. The colloids were introduced in a Fischer–Porter bottle. The reactor was pressurized with 3 bars of H_2 for 14 h to eliminate oxygen from the nanoparticles' surface. The gas was then evacuated under vacuum for 15 min, and the Fischer–Porter bottle further pressurized with 0.5 or 1 bar of ^{13}CO for different reaction times. Then, the ^{13}CO gas was evacuated under vacuum for 20 min and solid state ^{13}C NMR and IRFT spectra (KBr pellets) were recorded.

Acknowledgements

The authors thank V. Collière and L. Datas for their help during experiments on TEM instruments managed by UPS-TEMSCAN. They also acknowledge financial support from the French national METSA network of CNRS and CEA for HREM experiments at CEMES. CNRS, ANR (Siderus project ANR-08-BLAN-0010-03), and INTERREG SUDOE (TRAIN2 project) are also thanked for financial support. The EXAFS experiments were carried out at the light source DORIS III at DESY, a member of the Helmholtz Association (HGF). The research leading to these results has received funding from the European Community's Seventh Framework Programme (FP7/2007-2013) under grant agreement no. 226716. P. Lara Muñoz is grateful to the Spanish Ministerio de Educación for a research contract.

Notes and references

1 (*a*) T. A. Yamamoto, S. Kageyama, S. Seino, H. Nitami, T. Nakagama, R. Horioka, Y. Honda, K. Ueno and H. Daimon, *Appl. Catal., A*, 2011, **396**, 68–75; (*b*) C.-H. Chen, L. S. Sarma, D. Y. Wang, F.-J. Lai, C.-C. A. Andra, S.-H. Chang, D. G. Liu, C.-C. Chen, J.-F. Lee and B.-J. Hwang, *ChemCatChem*, 2010, **2**, 159–166; (*c*) T.-Y. Chen, T.-L. Lin, T.-J. M. Luo, Y. Choi and J.-F. Lee, *ChemPhysChem*, 2010, **11**, 2383–2392; (*d*) A. Murthy and A. Manthiram, *Electrochem. Commun.*, 2011, **13**, 310–313; (*e*) Y.-C. Wei, C.-W. Liu, W.-J. Chang and K.-W. Wang, *J. Alloys Compd.*, 2011, **509**, 535–541; (*f*) M. Liu, J. Zhang, J. Liu and W. W. Yu, *J. Catal.*, 2011, **278**, 1–7; (*g*) T.-Y. Jean, K.-S. Lee, S.-J. Yoo, Y.-H. Cho, S.-H. Kang and Y.-E. Sung, *Langmuir*, 2010, **26**, 9123–9129.

2 S. Sun, C. B. Murray, D. Weller, L. Folks and A. Moser, *Science*, 2000, **287**, 1989–1992.

3 (*a*) K. Philippot and B. Chaudret, *C. R. Chim.*, 2003, **6**, 1019–1034; (*b*) K. Philippot and B. Chaudret, in *Comprehensive Organometallic Chemistry III*, ed. R. Crabtree and M. P. Mingos, Elsevier, 2007.

4 (*a*) J. García-Antón, M. R. Axet, S. Jansat, K. Philippot, B. Chaudret, T. Pery, G. Buntkowsky and H. H. Limbach, *Angew. Chem., Int. Ed.*, 2008, **47**, 2074–2078; (*b*) F. Novio, K. Philippot and B. Chaudret, *Catal. Lett.*, 2010, **140**, 1–7.

5 (*a*) C. Pan, F. Dassenoy, M.-J. Casanove, K. Philippot, C. Amiens, P. Lecante, A. Mosset and B. Chaudret, *J. Phys. Chem. B*, 1999, **103**, 10098–10101; (*b*) F. Dassenoy, M.-J. Casanove, P. Lecante,

C. Pan, K. Philippot, C. Amiens and B. Chaudret, *Phys. Rev. B: Condens. Matter*, 2001, **63**, 235407–235414.
6 D. Ciuculescu, C. Amiens, M. Respaud, A. Falqui, P. Lecante, R. E. Benfield and B. Chaudret, *Chem. Mater.*, 2007, **19**, 4624–4626.
7 (*a*) T. Pery, K. Pelzer, G. Buntkowski, K. Philippot, H. H. Limbach and B. Chaudret, *ChemPhysChem*, 2005, **6**, 605–607; (*b*) F. Schröder, D. Esken, M. Cokoja, M. W. E. Van den Berg, O. Lebedev, G. Van Tendeloo, B. Walaszek, G. Buntkowsky, H.-H. Limbach, B. Chaudret and R. A. Fischer, *J. Am. Chem. Soc.*, 2008, **130**, 6119–6130; (*c*) A. Adamczyk, Y. Xu, B. Walaszek, F. Roelofs, T. Pery, K. Pelzer, K. Philippot, B. Chaudret, H.-H. Limbach, H. Breitzke and G. Buntkowsky, *Top. Catal.*, 2008, **48**, 75–83; (*d*) L. A. Truflandier, I. Del Rosal, B. Chaudret, R. Poteau and I. C. Gerber, *ChemPhysChem*, 2009, **10**, 2939–2942.
8 (*a*) M. Lersch and M. Tilset, *Chem. Rev.*, 2005, **105**, 2471–2526; (*b*) I. M. Ciobica, A. W. Kleyn and R. A. Van Santen, *J. Phys. Chem. B*, 2003, **107**, 164–172.
9 R. Berthoud, A. Baudouin, B. Fenet, W. Lukens, K. Pelzer, J. M. Basset, J. P. Candy and C. Copéret, *Chem.–Eur. J.*, 2008, **14**, 3523–3526.
10 (*a*) D. de Caro and J. S. Bradley, *Langmuir*, 1998, **14**, 245–247; (*b*) D. de Caro and J. S. Bradley, *New J. Chem.*, 1998, 1267–1273; (*c*) J. Grunes, J. Zhu, M. C. Yang and G. A. Somorjai, *Catal. Lett.*, 2003, **86**, 157–161; (*d*) A. M. Contreras, J. Grunes, X.-M. Yan, A. Liddle and G. A. Somorjai, *Catal. Lett.*, 2005, **100**, 115–124; (*e*) A. M. Contreras, J. Grunes, X.-M. Yan, A. Liddle and G. A. Somorjai, *Top. Catal.*, 2006, **39**, 123–129; (*f*) P. Deshlahra, K. Pfeifer, G. H. Bernstein and E. E. Wolf, *Appl. Catal., A*, 2011, **391**, 22–30.
11 (*a*) S. E. Shore, J. P. Ansermet, C. P. Slichter and J. H. Sinfelt, *Phys. Rev. Lett.*, 1987, **58**, 953–956; (*b*) J. P. Ansermet, C. P. Slichter and J. H. Sinfelt, *J. Chem. Phys.*, 1988, **88**, 5963–5971; (*c*) L. R. Becerra, C. A. Klug, C. P. Slichter and J. H. Sunfelt, *J. Phys. Chem.*, 1993, **97**, 12014–12019.
12 A. Duteil, R. Quéau, B. Chaudret, R. Mazel, C. Roucau and J. S. Bradley, *Chem. Mater.*, 1993, **5**, 341–347.

